Snow-darkening versus direct radiative effects of mineral dust aerosol on the Indian summer monsoon onset: role of temperature change over dust sources

Zhengguo Shi[1, 2, 3], Xiaoning Xie[1], Xinzhou Li[1, 2], Liu Yang[1], Xiaoxun Xie[1], Jing Lei[1], Yingying Sha[1], and Xiaodong Liu[1, 2]

[1]State Key Laboratory of Loess and Quaternary Geology, Center for Excellence in Quaternary Science and Global Change, Institute of Earth Environment, Chinese Academy of Sciences, Xi'an 710061, China
[2]CAS Center for Excellence in Tibetan Plateau Earth Sciences, Beijing 100101, China
[3]Open Studio for Oceanic-Continental Climate and Environment Changes, Qingdao National Laboratory for Marine Science and Technology, Qingdao, China

Correspondence to: Dr. Zhengguo Shi (shizg@ieecas.cn)

Abstract. Atmospheric absorptive aerosols exert complicated effects on the climate system and two of which are through their direct radiative forcing and snow-darkening forcing. Compared to black carbon, the snow-darkening effect of dust on climate has been scarcely explored till now. When depositing in snow, dust can reduce the albedo of snow by darkening it and increase the snow melt. In this study, the snow-darkening effect of dust, as well as the direct radiative effect, on the Indian summer monsoon are evaluated by atmospheric general circulation model experiments. The results show that, the snow-darkening and direct radiative forcing of dust have both significant impacts on the onset of Indian monsoon but they are distinctly opposite. The snow-darkening effect of dust weakens the Indian monsoon precipitation during May and June, opposite to black carbon. The surface temperature over Central Asia and western Tibetan Plateau becomes warmer due to the dust-induced decrease in snow cover, which leads to a local low-level cyclonic anomaly as well as an anticyclonic anomaly over Indian subcontinent and Arabian Sea. This circulation pattern allows air current penetrating into Indian subcontinent more from Central Asia but less from Indian Ocean. In contrast, the direct radiative forcing of dust warms the low troposphere over Arabian Peninsula, which intensifies moisture convergence and precipitation over Indian monsoon region. The upper tropospheric atmospheric circulation over Asia is also sensitive to both effects. Compared to previous studies which emphasized the temperature over Tibetan Plateau, our results further highlight an important role of surface/low tropospheric temperature changes over dust source areas, which can also significantly modifies the response of summer monsoon. Thus, links between the climatic impact of dust and complicated thermal condition over Asia are of importance and require to be clarified accurately.

1 Introduction

Mineral dust, a kind of natural aerosols in the atmosphere, mainly originates from the global deserts including Sahara, Arabian peninsula, Central Asia and East Asia. Dust emitting into the atmosphere is carried by atmospheric circulation and can be transported downwind for a long distance (Zhang et al., 1997; Zhao et al., 2006; Kallos et al., 2006; Schepanski et al., 2009; Shi and Liu, 2011). Mineral dust aerosol affects global and regional energy budget, formation of clouds and precipitation as well as various climate systems through their direct, semi-direct and indirect effects (e.g., Tegen and Lacis, 1996; Ramanathan et al., 2001; Miller et al., 2004; Shao et al., 2011; Huang et al., 2014; Mahowald et al., 2014). Among the climatic effects of dust, the direct radiative effect (DRE) and snow-darkening effect (SDE) are two important components, which exert great impacts on the radiative balance (Haywood et al., 2001; Flanner et al., 2009; Huang et al., 2014; Qian et al., 2015).

The DRE of dust is that the particles can directly scatter and absorb the solar shortwave and black-body longwave radiation. In the fifth Assessment Report (IPCC, 2013), the annual mean DRE of dust is approximately -0.10 W m^{-2} on the global scale, which varies from -0.30 to $+0.10$ W m^{-2} among different global climate models. However, it is still unclear whether dust aerosol has a net warming or cooling effect on global climate (e.g., Tegen and Lacis, 1996; Miller and Tegen, 1998; Mahowald et al., 2014; Kok et al., 2017; Xie et al., 2018a). Due to the underestimation of coarser dust in climate models than in the atmosphere, the considered DRE may be more cooling in current model ensemble and the possibility that dust causes a net warming is highlighted (Kok et al., 2017).

Following the changes in radiative balance, specific climate systems or atmospheric circulations also respond significantly to the DRE of aerosols. During the emission seasons, dust from inland Asian and Arabian deserts is delivered downwind by the westerlies and Asian monsoon (Uno et al., 2009; Shi and Liu, 2011; Vinoj et al., 2014) to eastern China, India and even deposits in the Tibetan Plateau (Huang et al., 2007; Xu et al., 2009; Zhang et al., 2018). Such distributions of atmospheric dust largely affect the Asian climate, including both Indian and East Asian monsoon (Lau et al., 2006; Zhang et al., 2009; Sun et al., 2012; Vinoj et al., 2014; Jin et al., 2014; Gu et al., 2016; Lau et al., 2017; Lou et al., 2017). Via a strong effect of elevated heat pump, the DRE of absorbing aerosols including dust enhances the heat source over the TP and results in a northward shift of Indian summer monsoon during the late spring and early summer (Lau et al., 2006; Lau et al., 2017). The aerosol-induced upper tropospheric warming intensifies the updraft air motion, which pumps more moist air from south oceans to north India. However, this hypothesis is still in debate that lacks of observational support (Nigam and Bollasina, 2010). Beside the TP warming, the tropospheric warming over Arabian Sea and surrounding regions due to mineral dust from Middle East can intensify the Indian summer monsoon and precipitation (Vinoj et al., 2014; Jin et al., 2014). In addition, the East Asian monsoon and the eastern precipitation are also significantly affected by dust that northeasterly wind anomaly over eastern China seems to weaken the monsoon circulation (Sun et al., 2012; Tang et al., 2018).

SDE is another important effect of dust on climate, which is not mentioned as intensively as the DRE. Light absorbing aerosols can darken the snow and reduce the surface albedo when deposited in snow, and it can also absorb the radiation and warm the snow surface, which both accelerates the melt process of snowpack (Hansen and Nazarenko, 2004; Xu et al., 2009; Lee et al., 2013; Qian et al., 2015). Due to the reduction of snow, the SDE of absorbing aerosols generally induces a net regional

warming over the snow cover areas. Black carbon, as the most important anthropogenic absorbing aerosols, has a global-mean radiative forcing of +0.04 (+0.02 to +0.09) W m^{-2} for SDE (Bond et al., 2013). Over the Tibetan Plateau (TP) where most areas are covered by snow, in particular, the absorbing aerosols in snow remarkably influence the snow albedo and promote the snowmelt (Lau et al., 2010; Yasunari et al., 2011; He et al., 2014; Zhao et al., 2014; Lee et al., 2017; Niu et al., 2017). The SDE of black carbon generates positive changes in surface radiative flux of about 5−25 W m^{-2} over the TP during springtime, warms the surface TP obviously and intensifies both the Indian and East Asian summer monsoon by enhancing the elevated heat source (Qian et al., 2011; Qian et al., 2015).

Compared to that of black carbon, the SDE of mineral dust over TP and Asia, especially its influence on the Asian monsoon, is still not clear. Theoretically, the SDE of dust is considered to be larger than that of black carbon over the TP (Flanner et al., 2009; Ming et al. 2013) primarily because the concentration of dust is much higher. The spatial distribution and deposition of dust is also different from black carbon that the dust can be deposited over both central Asia and TP where exists a fraction of snow cover while black carbon is primarily restricted to South and East Asia and downwind areas. In actual, the dust is a kind of natural aerosols, differing from black carbon which is mainly anthropogenic produced. Beside the modern period, the climatic effect of Asian dust are also of great importance in the geological stages, such as the last glacial maximum (Harrison et al., 2001; Claquin et al., 2003; Takemura et al., 2009). During the late Cenozoic, the dust effect ought to become gradually larger as deserts expand and atmospheric dust increases with plateau uplift and climatic cooling (Shi et al., 2011). Thus, it is necessary to explore in detail the effect of dust during present day and geological periods.

In this paper, as a first step, we employed a set of numerical experiments by a general circulation model to evaluate the SDE and DRE of dust on Indian summer monsoon during the onset under present-day conditions. In Section 2, the model and experiments are described. The model performance, response of Indian monsoon and role of temperature changes over dust sources are presented in Section 3. The discussion and conclusions are summarized in Section 4 and 5, respectively.

2 Model and Experiments

An atmospheric general circulation model namely Community Atmosphere Model 4 (CAM4), which is improved with a new bulk aerosol model (BAM) parameterization, is employed to evaluate the response of Indian summer monsoon to the forcing of mineral dust. CAM4 is the atmospheric component of the Community Climate System Model 4 (CCSM4), which is coupled with the Community Land Model 4 (CLM4) for land surface processes. The vertically Lagrangian and horizontally Eulerian coordinates are used in the finite-volume discretization of this model. The dust cycle including the emission, transport and deposition, is parameterized in CAM4 and its radiative feedbacks are also calculated on line. The dust sizes in CAM4 contain four bins of 0.1−1.0 μm, 1.0−2.5 μm, 2.5−5.0 μm and 5.0−10.0 μm in diameters, respectively (Mahowald et al., 2006). The CAM4-BAM has been improved by an optimized soil erodibility map and a new size distribution for dust emission (the percentages for four bins are 0.02, 0.09, 0.27, 0.62, respectively), as well as updated optical properties for radiation budget, to present a better performance on simulating the global dust cycle (Albani et al., 2014). In CAM4-BAM, the SDE of all aerosols are enabled but the indirect effect is not considered, which means that the aerosol changes in cloud process as condensation

nuclei are prescribed. Wet removal through in-cloud process is not considered, which may induce bias of dust deposition on snow over Asia. The snow darkening processes are considered based on the Snow, Ice and Aerosol Radiative (SNICAR) module (Flanner et al., 2007; 2009) in which the dust and black carbon aerosols are included. The SNICAR applies Mie scattering to particle mixture and a multi-layer radiative transfer approximation (Toon et al., 1989) to represent vertical inhomogeneity in the snow. The radiative transfer in the snow is affected by the vertical particle profile controlling by fresh snow and flushing with melt water when dust deposits on the surface. Dust optical properties in snow were ranging from 0.88 to 0.99 with decreasing particle size (Flanner et al., 2009). Of note is that SCINAR assumes external mixing between aerosols and spherical snow grains, however, aerosol-snow internal mixing and nonspherical snow shape could significantly affect aerosol-induced snow albedo effects, based on recent studies (Flanner et al., 2012; Liou et al., 2014; Räisänen et al., 2017; He et al., 2018).

Three sensitivity experiments are conducted in this study to evaluate the SDE and DRE of mineral dust. Both the snow-darkening and direct radiative effects of dust are turned on in the experiment namely EXP1d while only the direct radiative effect is enabled in the experiment of EXP2d. Neither effects are taken into consideration in the third experiment (EXP3d). Thus, the differences in climate responses between EXP1d and EXP2d, and between EXP2d and EXP3d, are denoted as the SDE and DRE of dust, respectively. Of note is that the dust column loading over Asia is slightly larger by the on-line feedbacks when both two effects are enabled, compared to that when DRE is only enabled. However, the bias does not affect our discussion, which will be mentioned later in this work. The reason for the intensified dust cycle over Asia by SDE is analyzed in detail in a parallel study (Xie et al., 2018b). Other species of aerosols except mineral dust are neglected in these experiments to avoid the biases induced by their different spatial distributions in different experiments. In order to compare with previous studies with a main focus on black carbon, three experiments on SDE and DRE of black carbon are also conducted (EXP1bc, EXP2bc and EXP3bc, respectively) and the design is similar. For these six experiments, the boundary conditions, including the sea surface temperature and greenhouse gas concentrations, are kept as their modern values (The year 2000 AD). The sea surface temperature and sea ice is given from HadOIBI data and the atmospheric CO_2 concentration is set to 367 ppmv.

In these experiments, the horizontal resolution of CAM4-BAM is set to approximately $0.9^\circ \times 1.25^\circ$ in latitude and longitude. All the experiments are integrated for a total period of 21 years and the results of the last 15 years are analyzed. Both monthly and daily mean values of variables are outputted to examine the sensitivity of monsoon. The response of Indian monsoon circulation and precipitation during May and June (i.e., the onset) is focused in this study since the monsoon onset is sensitive to external thermal forcing. Due to the limit of calculation resource, we only conducted atmospheric model experiments in this study and coupled ocean-atmosphere model experiments are not included. Actually, slow ocean response can play a dominant role in the response of Indian summer monsoon to aerosol forcing (Ganguly et al., 2012).

3 Results

3.1 Model validation

Before the examination of monsoon response, the model's ability on simulating the climatology of dust aerosol optical depth (AOD), snow cover and Indian monsoon during May and June in the experiment EXP1d is first evaluated using modern

observation and reanalysis data. The distributions of the AOD and deposition flux of mineral dust in the model over Asia are shown (Figure 1). The maximal values of May-June mean dust AOD are found over the arid and semi-arid regions including the Sahara, Arabian Peninsula, Central Asian and East Asian deserts (Figure 1a). The AOD reaches above 0.2 over major source areas. This simulated pattern is similar with the Cloud-Aerosol Lidar and Infrared Pathfinder Satellite Observation (CALIPSO)-retrieved AOD over the deserts (Figure 1b), which indicates that CAM4-BAM has a good performance on the dust cycle. The simulated absolute values of dust AOD over Arabian Peninsular, southwestern slope of the TP and Taklimakan desert are biased low because the considered dust particles are restricted to less than 10.0 μm and the dust forcing is underestimated due to less coarser dusts in the current global climate models (Kok et al., 2017). The total deposition fluxes during April and May-June (Figures 1c, 1d) show that there are remarkable dust depositions over Asia and adjacent oceans in both periods. In April, the dust deposition over East and Central Asian deserts and downwind regions is larger than that in May and June. In contrast, the deposition over Arabian Peninsula is more obvious in May and June, which is also detected over Arabian Sea and western Indian continent. Over the western and northeastern Tibetan Plateau (TP), the deposition flux is simulated with a range of about 0.02-0.16 kg/m^2/yr.

The simulated snow cover fractions over Asia during May to June show that surface snow exists over Central Asia, East Asia and the whole TP, with largest fractions over western TP (Figure 2a). In Moderate Resolution Imaging Spectroradiometer (MODIS) data, the observed snow cover is found over the same regions that maximal values are located over Mongolia, western and southeastern TP (Figure 2b), which is qualitatively consistent with that in the EXP2d simulation. Over the western TP, the MODIS observation presents a fraction larger than 80% but the simulated fraction is smaller. In particular, the model underestimates the elevations of finer-scale mountains and corresponding snow cover fractions due to the coarser resolution, e.g., over the Tianshan mountains. In April, the snow cover fractions over Central Asia and TP are larger than those in May to June (Figure 2c, 2d). Over TP, the amplitudes are similar for both simulation and observation but around Caspian Sea the simulated values are smaller. The dust deposition in the surface snow over Asia implies a potential influence on surface snow.

For the Indian monsoon climatology, a feature that the monsoon westerly winds are divided into two branches (e.g., Wu et al., 2012), with the northern one from Central Asian dry regions and southern one from moist Indian Ocean, is simulated in the 850hPa winds during May and June (Figure 3a). During the monsoon onset, the southerly winds over this region gradually develop from the south to the north. During the same period, the Indian monsoon precipitation is mainly produced over the western sides of the Indian and Indo-China peninsulas as well as the southern slope of the TP (Figure 3c). These features of Indian monsoon circulation and precipitation are generally in agreement with the National Centers for Environmental Prediction/National Center for Atmospheric Research (NCEP/NCAR) reanalysis and Tropical Rainfall Measuring Mission (TRMM) satellite-retrieved data (Figures 3b, 3d). Compared to the observations, the simulated precipitation is lighter over the western sides of two peninsulas but heavier over the southern slope of the TP. In brief, CAM4-BAM performs well in both the monsoon climatology and dust cycle over Asia, which builds confidence for assessing the climate sensitivity to dust forcing.

3.2 Response of Indian monsoon

The daily precipitation differences during May and June between EXP1d and EXP2d, as well as between EXP2d and EXP3d, are calculated to examine the responses of monsoon onset to SDE and DRE of dust (Figure 4). It is clearly seen that in all three experiments the precipitation rates over Indian monsoon area (10-25°N, 65-100°E) increase abruptly by an amount of approximately 10 mm day^{-1} during several weeks in the onset (Figure 4a). In this two-month period, the dust SDE-induced difference is mostly negative while the dust DRE-induced difference is positive (Figure 4b), which means that the SDE tends to weaken the Indian summer monsoon but the DRE likes to intensify it. This is also the reason why we choose May and June as the monsoon onset in the following analysis. The SDE-induced precipitation decrease exceeds the DRE-induced increase in June, which results in a net reduction in precipitation; however, these two effects almost counteracts by each other and the total precipitation change in May is not significant.

The spatial distributions of May-June mean precipitation show that the precipitation rate is decreased by the SDE over most Indian monsoon regions and a remarkable difference by 1 mm day^{-1} is detected over India (Figure 5a). Other regions with statistically-significant precipitation changes are found over western and southeastern TP, parts of Central Asia and northeastern Africa. For DRE-induced response, the precipitation is promoted over Indian peninsula, Arabian Sea and Central Asia but suppressed over Bay of Bengal and southeastern TP (Figure 5b). Thus, the responses of Indian monsoon precipitation to the SDE and DRE are distinctly different during the onset, which highlights the complicated influence of mineral dust. The surface temperature becomes warmer over most Asia, which responds to the SDE (Figure 5c). The most obvious warming, with an amplitude of larger than 1°C, is found over the whole western TP where the surface snow cover is larger, which indicates that the SDE is significant at these regions. Another significant warming center is around Caspian Sea in Central Asia also with certain snow covers at this time. In contrast, the surface temperature difference induced by the DRE is significantly negative over the whole TP and northeastern India (Figure 5d). However, it is simulated to be warming over surface and low-level troposphere over Arabian Peninsula/Middle East (Figure 5d, S1a), which amplifies the zonal thermal gradient over Indian monsoon region.

The responses of Indian monsoon circulation to the SDE and DRE of dust are examined by the differences in 850 hPa wind vectors between experiments (Figures 6a, 6b). In the SDE-induced difference, a significant cyclonic anomaly is simulated over western TP and to its west there is also a cyclonic anomaly around the Caspian Sea (Figure 6a), following the surface temperature changes (Figure 5c). These two cyclonic anomalies tends to intensify the northern branch of Indian monsoon westerly, allowing more dry air from Central Asia penetrating into the monsoon region. However, the southern branch of the monsoon westerly is significantly decreased with the associated anticyclonic anomaly over Arabian Sea and India, which weakens the moisture transport from oceans in the south. This circulation anomaly over monsoon area agrees well with the simulated lighter precipitation, which supports that the Indian summer monsoon is weakened by the SDE during its onset. In addition, the westerly winds become stronger to the north of the TP, which might affect the dust emission further over that region. In the DRE-induced difference, the situation is quite different that a low pressure anomaly (Figure S1b) and corresponding cyclonic anomaly (Figure 6b) are simulated over the Arabian Peninsula in low troposphere, in response to

the surface and low level warming (Figure 5d, S1a). The northern branch of monsoon westerly is remarkably reduced in its intensity across the southern slope of the TP, the Persian Gulf and northern Arabian Peninsula (Figure 6b). The southern branch of Indian monsoon westerly over the Arabian Sea is simulated to be stronger, which intensifies the water vapor transport from oceans (Figure S1c). The westerly winds are also decreased over the Bay of Bengal and Indo-China Peninsula, however, it brings water vapor to the Indian Peninsula. The differences in the moisture convergence induced by the SDE and DRE show that the water vapors diverge and converge over most Indian monsoon region, respectively (Figures 6c, 6d), consistent with the responses of precipitation (Figures 5a, 5b).

Compared to the dust, the SDE and DRE of black carbon on the Indian summer monsoon onset are also analyzed (Figure S2, S3). The black carbon's SDE-induced surface temperature change is similar with dust but is restricted to western TP with no warming over Central Asia (Figure S2a). The TP warming intensifies the Indian monsoon and leads to strong anomaly in southerly winds over India, which subsequently brings more rainfall over this region (Figure S2b, S2c). The SDE of black carbon is distinctly different with that of dust, which indicates the complicated SDE of absorbing aerosols on Indian monsoon not mentioned before. For the DRE of black carbon, a surface warming over western TP is simulated (Figure S3a). The warming is also over Pakistan and Afghanistan although it is not significant. This effect strengthens the southwesterly winds over the Arabian Sea and moisture transport from ocean (Figure S3b) and the precipitation is intensified over the Arabian Sea and southern India (Figure S3c). Thus, the SDE and DRE of black carbon are consistently to intensify the Indian monsoon during the onset.

The responses of Indian monsoon in high-troposphere is examined (Figure 7) because the anomalous heating center over the TP as well as the high pressure cell are both important for the monsoon development. As seen in the 200 hPa climatology, a SDE-induced dipole pattern of meridional temperature changes over Central Asia and TP (Figure 7a) results in a western weakening and a eastern strengthening of South Asian high pressure cell, i.e., a eastward shift of high pressure cell (Figure 7c). In contrast, the opposite dipole temperature changes caused by DRE make the high pressure cell move westward (Figures 7b, 7d). The strong Arabian Peninsular warming over high troposphere is in agreement with the surface (Figure 5d), which indicates that this warming is significant throughout the column atmosphere. Differences in 200 hPa wind vectors also show a couple of reversed circulation changes of cyclonic/anticyclonic cell in the west and anticyclonic/cyclonic cell in the east responding to the SDE and DRE, respectively (Figures 7e, 7f), consistent with the temperature and pressure changes. To the north of the TP, the westerly winds are weakened by the SDE, which might help the long-distance transport of mineral dust over East Asia.

Changes in vertical motion show that low and middle tropospheric subsidence occurs over most of the monsoon areas with the SDE but the DRE leads to ascending motion over Arabian Sea and western India (Figure 8). Strong ascending motion due to the SDE is found over the TP and Caspian Sea (Figure 8a, 8c), which is closely linked with local surface warming (Figure 5c). In contrast, the subsidence dominates the adjacent areas outside the TP including the Indian and Indo-China peninsulas, as well as regions to the west and north of the TP (Figure 8a, 8c), which is in good agreement with low-level circulation changes (Figure 6a). For the DRE, the ascending motion is presented over northern India although surface cooling produces local subsidence over the TP (Figure 8d). The spatial distributions of anomalous vertical motion over Indian monsoon region are in

qualitatively coincidence with the simulated precipitation changes by SDE and DRE, respectively. Such circulation changes is also clearly seen in the cross sections for vertical versus meridional winds (not shown).

From the analysis above, in brief, the suppressed and increased monsoon precipitation during May and June are fundamentally resulted from the SDE and DRE induced changes in atmospheric temperature structure, respectively, especially over the low-level atmosphere where most mineral dust exists. Compared to black carbon, the SDE effect of dust is opposite because the range for dust-induced temperature increase does not only occupy over western TP but also expands to central Asia, which indicates the role of central Asian temperature changes in modulation of SDE on the monsoon. Although the DRE of dust is similar with that of black carbon, the simulated surface temperature changes over the TP are distinctly different. In our sensitivity runs, the intensified monsoon by dust DRE is more likely ascribed to the low tropospheric atmospheric warming over Arabian Peninsula. Thus, the potential importance of temperature changes over dust sources (i.e., Central Asia and Arabian Peninsula, respectively) is highlighted in SDE and DRE of dust.

The possible reasons for the SDE- and DRE-induced low tropospheric temperature changes over dust source areas are analyzed from a perspective of energy budget. The SDE-induced differences in longwave and shortwave radiation fluxes for all-sky conditions during May and June at the top of atmosphere (TOA), at the surface and in the column atmosphere are shown in Figure 9. For both the TOA and the surface, the primary forcing of SDE is via shortwave radiation change since it is albedo-induced. Due to large snow cover, the strongest shortwave radiation change is found positive over western TP and Mongolia (Figures 9b, 9e), which indicates that both the TOA and the surface receive more shortwave radiation while the scattering becomes less. The positive shortwave forcing near Indian Peninsula, not so strong as that over TP, is offset by the negative longwave one (Figures 9a, 9d), in which these changes should be associated with internal adjustment of climate, e.g., the water vapor change. As a result, the SDE totally means a positive net radiative forcing over western TP at the TOA and the surface (Figures 9c, 9f), which is the reason for local surface warming (Figure 5c). Additionally, the net surface and column radiative forcing is also positive and statistically significant to the south of Caspian Sea, which contributes partly to the warming over this region, although its absolute value is not as large as that over western TP (Figure 9f, 9i). However, the change in surface shortwave radiative forcing is not visible over Central Asia (Figure 9e), indicating that the SDE over this region is not significant during May and June. For the column atmosphere, the shortwave radiation flux does not vary, supporting that the slight dust loading difference between EXP1d and EXP2d merely presents negligible radiation changes. The negative longwave radiation difference is merely found near Indian Peninsula (Figures 9g, 9h, 9i), indicating that the atmosphere loses energy over this region.

For the DRE, the radiative forcing is characterized by positive longwave and negative shortwave radiation differences at both the TOA and the surface (Figures 10a, 10b, 10d, 10e) owing to the absorbing and scattering of radiation by dust. However, the TOA changes are less evident than the surface changes because the dust aerosol is primarily distributed in the low level. Notably, a significant difference of larger than 20W/m^2 in shortwave radiation is seen over western TP (Figures 10b, 10e), highlighting potential feedback of snow albedo. The net surface forcing is also positive over Arabian Peninsula but not statistically significant. Further, the positive net TOA forcing is obvious over Arabian Peninsula (Figures 10c, 10f), which indicates that the pattern of surface air temperature change by the DRE (Figure 5d) is more likely controlled by the TOA radiation change.

As absorbing aerosol, the longwave and shortwave forcing for the column atmosphere is negative and positive, respectively (Figures 10g, 10h), with maximal values distributed over the large dust AOD region (Figure 1a). The positive net total forcing of dust is found remarkably positive over Arabian Peninsula but not so large over East Asia (Figure 10i), which explains the simulated low-level tropospheric warming over Arabian Peninsula (Figure S1a).

Changes in surface sensible and latent heat fluxes over Asia due to the SDE and DRE of dust are shown, respectively (Figure 11). For the SDE, the sensible heat flux obviously increases over western TP and near Caspian Sea areas (Figure 11a). The increase in sensible heat flux is found in good agreement with the surface warming (Figure 5c), which indicates that the sensible heat helps to explain the surface warming, especially over Central Asia. The latent heat flux also increases over western TP but decreases over Central Asia (Figure 11b). As a result, the simulated TP warming is actually from changes in radiation, sensible and latent heat; in contrast, the Central Asia warming around Caspian Sea is mainly from sensible heat changes. For the DRE, the sensible heat is negative but the latent heat is positive over all the source areas (Figure 11c, 11d). Both of the heat fluxes over the TP is negative due to the snow-induced feedback.

The reason for the sensible heat change by SDE is shown in the responses of surface ground temperature and snow cover fraction (Figure 12). Consistent with surface air temperature and sensible heat flux, the surface ground temperature is also increased by larger than 0.5°C and statistically significant over western TP and near Caspian Sea areas (Figure 12a). Responsible for increased sensible heat fluxes over these regions, the large ground temperature change is resulted from the decrease in surface snow covers (Figure 12b, 12c). However, the snow cover change over Central Asia is different from that over western TP. In May and June, the snow covers over TP are significantly decreased by the SDE but those over Central Asia do not vary (Figure 12b). In contrast, the snow covers around Caspian Sea become less in April (Figure 12c) and the decreased snow covers share a similar pattern with the local ground temperature (Figure 12a). The ground warming over Central Asia during May and June is actually controlled by the snow cover change in April and this delayed response of ground temperature is possibly due to the thermal inertia of land. These seasonal differences in Central Asian snow covers are also in good agreement with the diagnostic surface forcing of dust-in-snow in model (Figure 13). In May and June, the forcing is merely restricted to western TP (Figure 13a), but in April, the forcing expands to the Caspian Sea areas (Figure 13b) and promotes the snow melt. Thus, the warming over Central Asia during May and June is primarily from the preceding SDE forcing. The SDE forcing in April induces a decrease in surface snow covers and then a delayed warming of ground temperature in May and June. The ground warming intensifies the sensible heat exchange and contributes significantly to the surface air temperature change. For black-carbon-in-snow, there is none surface forcing over Central Asia during both April and May-June (Figure S4), highlighting their spatial differences in SDE between black carbon and dust.

4 Discussion

The physical mechanisms for SDE and DRE of mineral dust on the Indian summer monsoon during the onset are summarized by schematic diagrams, respectively (Figure 14). The forcing of SDE occurs over western TP and Central Asia, which becomes warmer due to decreased snow cover. Subsequently, two anomalous surface low pressure centers are produced and upward air

flow dominates over these areas (Figure 14a). To their south, a forced high pressure and anticyclone anomaly is found over Bay of Bengal and India where the subsidence suppresses the formation of monsoon rainfall. For the circulation, the anticyclone strengthens the westerly air flow from the dry Central Asia but limits that from moist Indian Ocean. In contrast, the forcing of DRE induces a low tropospheric warming over Arabian Peninsula, which produce a low pressure anomaly (Figure 14b). Such a pattern gives a SDE-opposite impact of circulation, which intensifies the cross-equatorial southerly and weakens the dry air flows from the north. The role of western TP cooling and high pressure anomaly is not certain considering that they are different from black carbon-induced changes.

The radiative forcing and remarkable TP warming at the surface and high troposphere, as a direct response to SDE of dust or other absorbing aerosols (e.g., black carbon), is also found in previous studies (Flanner et al., 2009; Lau et al., 2010; Qian et al., 2011). They proposed that the snowmelt process is rapid and efficient during the late spring and early summer (Lau et al., 2010; Qian et al., 2011; Qian et al., 2015) and this sensitive response of snow cover to SDE in melting season supports its significant role in Indian monsoon development simulated in this study. Change in thermal condition over surface TP, which acts as a heat source and exerts great sensible heat flux to atmosphere, are proved to be essential in the establishment of Indian monsoon (e.g., Yanai et al., 1992; Li and Yanai, 1996; Liu et al., 2001). Furthermore, change in snow cover over TP can also obviously affect the Indian monsoon by modifying the thermal TP forcing (e.g., Vernekar et al., 1994; Senan et al., 2016) and those over different parts of TP may play different roles (Wang et al., 2017). The response of Indian monsoon to SDE of black carbon during the onset (Qian et al., 2011, hereafter Qian2011) is similar from what we found here for black carbon. As a result, it seems that the SDE of dust in this study is reasonable although it is different from black carbon. Qian2011 emphasized that the polluted snowpack by black carbon over the TP warms the local surface and enhances the sensible heat flux, which results in a earlier onset of Indian monsoon and heavier precipitation over northern India. The opposite monsoon response to dust originate from different locations of surface warming that the warming due to black carbon is just over the TP but the warming due to dust extends quite westward to Central Asia.The westward extension of warming forces the southerly winds over India (See Figure S2 in this study and Figure 15c in Qian2011) to Arabian Peninsula (Figure 6a). Black carbon, mainly emitted from the Industrial countries, is generally transport eastwards and scarcely into upwind Central Asia. These differences in surface warming by dust and black carbon are also simulated in the experiments by NASA Goddard Earth Observing System Model (Yasunari et al., 2015). We agree that the importance of TP temperature proposed in SDE of absorbing aerosols and TP temperature is certainly vital for the Indian summer monsoon development (Qian et al., 2011), from a general perspective, although the responses to dust and black carbon have each features. Our results further promotes the complexity of monsoon response to temperature pattern because Central Asia is one of the dust sources and also covered by snow. If a perturbance indeed occurs over this region, it may modulate the response of monsoon to TP warming.

The DRE-strengthened Indian summer monsoon in this paper is in qualitatively agreement with previous studies (Lau et al., 2006, hereafter Lau2006; Gu et al., 2016; Lau et al., 2017), in which either dust or black carbon, or both of them, is included. However, the results may share different mechanisms. For example, the DRE-strengthened Indian summer monsoon in Lau2006 by both dust and black carbon is ascribed to an elevated heat pump (EHP) mechanism that the aerosols heat the southern slope of TP by absorbing the radiation and the hot air rises, which draws in moisture convergence over India. In our

black carbon experiments, consistent response of Indian monsoon is simulated although the 3D distribution of black carbon is different. However, the EHP mechanism fails to be obvious when only mineral dust is considered here, because the DRE of dust only induces a remarkable surface cooling over TP during May and June not a warming as shown in our black carbon experiment and Lau2006. The TP warming in Lau2006 is more likely induced by black carbon and we do not make sure whether it can be produced by dust only. Interestingly, there are consistent intensified summer monsoon and upward air motion over northern India in these studies (Lau et al., 2006; Gu et al, 2016). In this study, the intensified summer monsoon due to dust is from low tropospheric warming over Arabian Peninsula (Figures 5d, S1a), which drives moisture from southern oceans to Indian monsoon areas. This mechanism gains support from previous researches (Vinoj et al., 2014; Jin et al., 2014; Solmon et al., 2015), which emphasized the modulation of western African dust on Indian monsoon rainfall. In our study, the western African dust warms the low-level troposphere and produces low pressure anomaly over Arabian Peninsula, which is in good agreement with their studies. The intensified high pressure cell in high troposphere over Arabian Peninsula is also emphasized in an observation study to affect the onset of Indian monsoon (Zhang et al., 2014). Worthy of being pointed out is that the DRE of dust on surface temperature is largely uncertain and depends closely on the size distributions, optical properties and etc (Kok et al., 2017), which restricts our accurate understanding of dust effect. The different performance of dust-induced radiative forcing and temperature changes over East Asia and northern Africa can be explained by different surface albedo background and particle sizes (Liu et al., 2008; Takemura et al., 2009; Su and Toon, 2011; Xie et al., 2018a).

5 Conclusions

In this study, significant responses of Indian summer monsoon, including both circulation and precipitation during the onset, are proposed to the SDE and DRE of mineral dust, which is closely associated with surface and/or tropospheric temperature changes over dust sources. The SDE and DRE of dust are found to exert different impacts on monsoon system due to distinct temperature changes over Asia, highlighting the complexity of climate effect of dust. The forcing mechanisms of dust effect and the responses of Indian monsoon may be also different from black carbon. Compared to black carbon-induced warming over only western TP, the SDE of dust warms the surface over both Central Asia and western TP, which weakens the monsoon development and precipitation during May and June. Different from the TP, the Central Asian warming is mainly resulted from the SDE-induced snow cover change in the preceding month, which warms the ground and intensifies the sensible heat exchange. The DRE of dust warms the low troposphere over Arabian Peninsula and intensifies the monsoon onset. As net result of SDE and DRE of dust, the precipitation in June is reduced. Beside the Indian monsoon, East Asian monsoon should be also affected by the dust-induced thermal change, which will be examined in future. Compared to black carbon presenting positive TOA forcing, the DRE of dust on atmospheric radiation budget and thermal structure are still uncertain, which adds difficulty to evaluate the sensitivity of specific climate system to dust effect. Nevertheless, the role of dust still requires to be deeply explored due that it is natural and ought to be important during past climate change. In particular, several times larger dust burden and deposition during the Last Glacial Maximum (Mahowald et al., 2006; Maher et al., 2010), as well as higher snow cover fraction due to cold climate, are likely to induce stronger DRE and SDE than present day.

Author contributions. ZS designed the research and analyzed the results. XiaonX and XL conducted the experiments. ZS prepared the manuscript with contributions from all co-authors.

Acknowledgements. The authors appreciate two reviewers for their insightful comments, which were of great help for the manuscript. This work was jointly supported by National Key Research and Development Program of China (2016YFA0601904), the National Natural Science Foundation of China (41888101, 41572160), and the Strategic Priority Research Program of Chinese Academy of Sciences (XDA20070103). Shi Z. also acknowledged the support of Youth Innovation Promotion Association CAS and "Light of West China" Program.

References

Albani, S., Mahowald, N. M., Perry, A. T., Scanza, R. A., Zender, C. S., Heavens, N. G., Maggi, V., Kok, J. F., and Otto-Bliesner, B. L.: Improved dust representation in the Community Atmosphere Model, J. Adv. Model. Earth Syst., 06, 541–570, doi:10.1002/2013MS000279, 2014.

Bond, T. C., Doherty, S. J., Fahey, D. W., Forster, P. M., Berntsen, T., Deangelo, B. J., Flanner, M. G., Ghan, S., Kächer, B., Koch, D., Kinne, S., Kondo, Y., Quinn, P. K., Sarofim, M. C., Schultz, M. G., Schulz, M., Venkataraman, C., Zhang, H., Zhang, S., Bellouin, N., Guttikunda, S. K., Hopke, P. K., Jacobson, M. Z., Kaiser, J. W., Klimont, Z., Lohmann, U., Schwarz, J. P., Shindell, D., Storelvmo, T., Warren, S. G., and Zender, C. S.: Bounding the role of black carbon in the climate system: A scientific assessment, J. Geophys. Res. Atmos., 118, 5380–5552, doi:10.1002/jgrd.50171, 2013.

Claquin, T., Reolandt, C., Kohfeld, K., Harrison, S., Tegen, I., Prentice, I., Balkanski, Y., Bergametti, G., Hansson, M., Mahowald, N., Rodhe, H., Schulz, M.: Radiative forcing of climate by ice-age atmospheric dust, Clim. Dyn., 20, 193–202, 2003.

Flanner, M. G., Liu, X., Zhou, C., Penner, J. E., and Jiao, C.: Enhanced solar energy absorption by internally-mixed black carbon in snow grains, Atmos. Chem. Phys., 12(10), 4699–4721, 2012.

Flanner, M. G., Zender, C. S., Randerson, J. T., and Rasch, P. J.: Present day climate forcing and response from black carbon in snow, J. Geophys. Res., 112, D11202, doi:10.1029/ 2006JD008003, 2007.

Flanner, M. G., Zender, C. S., Hess, P. G., Mahowald, N. M., Painter, T. H., Ramanathan, V., and Rasch, P. J.: Springtime warming and reduced snow cover from carbonaceous particles, Atmos. Chem. Phys., 9, 2481–2497, doi:10.5194/acp-9-2481-2009, 2009.

Ganguly, D., Rasch, P.J., Wang, H., and Yoon, J.: Fast and slow responses of the South Asian monsoon system to anthropogenic aerosols, Geophys. Res. Lett., 39, https://doi.org/10.1029/2012GL053043, 2012.

Gu, Y., Xue, Y., De Sales, F., and Liou, K. N.: A GCM investigation of dust aerosol impact on the regional climate of North Africa and South/East Asia, Clim. Dyn., 46, 2353–2370, 2016.

Hansen, J. and Nazarenko, L.: Soot climate forcing via snow and ice albedos, P. Natl. Acad. Sci. USA, 101(2), 423–428, 2004.

Harrison, S. P., Kohfeld, K. E., Roelandt, C., Claquin, T.: The role of dust in climate changes today, at the last glacial maximum and in the future, Earth Sci. Rev., 54, 43–80, 2001.

Haywood, J. M., Francis, P. N., Glew, M. D., Taylor, J. P.: Optical properties and direct radiative effect of Saharan dust: A case study of two Saharan dust outbreaks dusing aircraft data, J. Geophys. Res.: Atmos., 106, 18417–18430, 2006.

He, C., Li, Q., Liou, K., Takano, Y., Gu, Y., Qi, L., Mao, Y., and Leung, L.: Black carbon radiative forcing over the Tibetan Plateau, Geophys. Res. Lett., 41, 7806–7813, 2014.

He, C., Liou, K., Takano, Y., Yang, P., Qi, L., and Chen, F: Impact of grain shape and multiple black carbon internal mixing on snow albedo: Parameterization and radiative effect analysis, J. Geophys. Res. Atmos., 123, 1253–1268, 2018.

Huang, J., Minnis, P., Yi, Y., Tang, Q., Wang, X., Hu, Y., Liu, Z., Ayers, K., Trepte, C., Winker, D.: Summer dust aerosols detected from CALIPSO over the Tibetan Plateau, Geophys. Res. Lett., 34, L18805, doi:10.1029/2007GL029938, 2007.

Huang, J., Wang, T., Wang, W., Li, Z., Yan, H.: Climate effects of dust aerosols over East Asian arid and semiarid regions, J. Geophys. Res. Atmos., 119, 11398–11416, doi: 10.1002/2014JD021796, 2014.

IPCC: Climate Change 2013: The Physical Science Basis. Contribution ofWorking Group I to the Fifth Assessment Report of the Intergovernmental Panel on Climate Change, edited by: Stocker, T. F., Qin, D., Plattner, G.-K., Tignor, M., Allen, S. K., Boschung, J., Nauels, A., Xia, Y., Bex, V., and Midgley, P. M., Cambridge University Press, Cambridge, United Kingdom and New York, NY, USA, 1535 pp., 2013.

Jin, Q., Wei, J., and Yang, Z.: Positive response of Indian summer rainfall to Middle East dust, Geophys. Res. Lett., 41, 4068–4074, 2014.

Kallos, G., Papadopoulos, A., Katsafados, P., and Nickovic, S.: Transatlantic Saharan dust transport: Model simulation and results, J. Geophys. Res.: Atmos., 111, D09204, doi: 10.1029/2005JD006207, 2006.

Kok, J. F., Ridley, D. A., Zhou, Q., Miller, R. L., Zhao, C., Heald, C. L., Ward, D. S., Albani, S., Haustein, K.: Smaller desert dust cooling effect estimated from analysis of dust size and abundance, Nature Geosci., 10, 274–278, doi:10.1038/ngeo2912, 2017.

Lau, K. M., Kim, K. M., Shi, J., Matsui, T., Chin, M., Tan, Q., Peters-Lidard, C., and Tao, W. K.:. Impacts of aerosol-monsoon interaction on rainfall and circulation over Northern India and the Himalaya Foothills, Clim. Dyn., 49, 1945–1960, 2017.

Lau, K. M., Kim, M. K., and Kim, K. M.:. Asian monsoon anomalies induced by aerosol direct forcing: the role of the Tibetan Plateau, Clim. Dyn., 26, 855–664, 2006.

Lau, K.-M., Kim, M. K., Kim, K.-M., and Lee, W. S.: Enhanced surface warming and accelerated snow melt in the Himalayas and Tibetan Plateau induced by absorbing aerosols, Environ. Res. Lett., 5, 025204 doi:10.1088/1748-9326/5/2/025204, 2010.

Lee, W.-L., Liou, K. N., He, C., Liang, H., Wang, T., Li, Q., Liu Z., and Yue, Q.: Impact of absorbing aerosol deposition on snow albedo reduction over the southern Tibetan plateau based on satellite observations, Theor. Appl. Climatol., 129, 1373–1382, 2017.

Lee, W. S., Bhawar, R. L., Kim, M. K., and Sang, J.: Study of aerosol effect on accelerated snow melting over the Tibetan Plateau during boreal spring, Atmos. Environ., 75, 113-122, 2013.

Li, C., and Yanai, M.: The Onset and Interannual Variability of the Asian Summer Monsoon in Relation to Land-Sea Thermal Contrast, J. Clim., 9, 358–375, 1996.

Liu, D., Wang, Z., Liu, Z., Winker, D., and Trepte, C.: A height resolved global view of dust aerosols from the first year CALIPSO lidar measurements, J. Geophys. Res., 113, D16214, https://doi.org/10.1029/2007JD009776, 2008.

Liu, X., and Yanai, M.: Relationship between the Indian monsoon rainfall and the tropospheric temperature over the Eurasian continent, Quart. J. Roy. Meteor. Soc., 127, 909-937, 2001.

Liou K. N., Takano, Y., He, C., Yang, P., Leung, L. R., Gu, Y., and Lee, W. L.: Stochastic parameterization for light absorption by internally mixed BC/dust in snow grains for application to climate models, J. Geophys. Res. Atmos., 119, 7616–7632, 2014.

Lou, S., Russell, L. M., Yang, Y., Liu, Y., Singh, B., and Ghan, S. J.: Impacts of interactive dust and its direct radiative forcing on interannual variations of temperature and precipitation in winter over East Asia, J. Geophys. Res., 122, 8761–8780, 2017.

Maher, B. A., Prospero, J. M., Mackie, D., Gaiero, D., Hesse, P., Balkanski, Y.: Global connections between aeolian dust, climate and ocean biogeochemistry at the present day and at the last glacial maximum, earth-sci. rev., 99, 61–97, doi:10.1016/j.earscirev.2009.12.001, 2010.

Mahowald, N. M., Muhs, D. R.,Levis, S., Rasch, P. J., Yoshioka, M., Zender, C. S., and Luo C.: Change in atmospheric mineral aerosols in response to climate: Last glacial period, preindustrial, modern, and doubled carbon dioxide climates, J. Geophys. Res., 111, D10202, doi:10.1029/2005JD006653, 2006.

Mahowald, N. M., Albani, S., Kok, J. F., Engelstaedter, S., Scanza, R., Ward, D. S., Flanner, M. G.: The size distribution of desert dust aerosols and its impact on the Earth system, Aeolian Res. 15, 53–71. http://dx.doi.org/10.1016/j.aeolia.2013.09.002, 2014.

Miller, R. L., and Tegen, I.: Climate response to soil dust aerosols, J. Clim., 11, 3247–3267, 1998.

Miller, R. L., Perlwitz, J., and Tegen, I.: Feedback upon dust emission by dust radiative forcing through the planetary boundary layer, J. Geophys. Res., 109, D24209, https://doi.org/10.1029/2004JD004912, 2004.

Ming, J., Wang, P., Zhao, S., and Chen, P.: Disturbance of light-absorbing aerosols on the albedo in a winter snowpack of Central Tibet, Journal of Environmental Sciences-China, 25(8), 1601–1607, doi: 10.1016/S1001-0742(12)60220-4, 2013.

Nigam, S., and Bollasina, M.: "Elevated heat pump" hypothesis for the aerosol-monsoon hydroclimate link: "Grounded" in observations? J. Geophys. Res., 115, D16201, doi: 10.1029/2009JD013800, 2010.

Niu, H., Kang, S., Zhang, Y., Shi, X., Shi, X., Wang, S., Li, G., Yan, X., Pu, T., and He, Y.: Distribution of light-absorbing impurities in snow of glacier on Mt. Yulong, southeastern Tibetan Plateau, Atmos. Res., 197, 474–484, 2017.

Qian, Y., Flanner, M., Leung, L., and Wang, W.: Sensitivity studies on the impacts of Tibetan Plateau snowpack pollution on the Asian hydrological cycle and monsoon climate, Atmos. Chem. Phys., 11(5), 1929–1948, doi: 10.5194/acp-11-1929-2011, 2011.

Qian, Y., Yasunari, T. J., Doherty, S. J., Flanner, M. G., Lau, W. K. M., Jing, M., Wang, H., Wang, M., Warren, S. G., and Zhang, R.: Light-absorbing Particles in Snow and Ice: Measurement and Modeling of Climatic and Hydrological impact, Adv. Atmos. Sci., 32, 64–91, doi:10.1007/s00376-014-0010-0, 2015.

Räisänen, P., Makkonen, R., Kirkevåg, A., and Debernard, J. B.: Effects of snow grain shape on climate simulations: Sensitivity tests with the Norwegian Earth System Model, The Cryosphere, 11, 2919–2942, 2017.

Ramanathan, V., Crutzen, P. J., Kiehl, J. T., and Rosenfeld, D.: Aerosols, climate, and the hydrological cycle, Science, 294, 2119–2124, 2001.

Schepanski, K., Tegen, I., and Macke, A.: Saharan dust transport and deposition towards the tropical northern Atlantic, Atmos. Chem. Phys., 9, 1173–1189, 2009.

Senan, R., Orsolini, Y. J., Weisheimer, A., Vitart, F., Balsamo, G., Stockdale, T. N., and Dutra, E.: Impact of springtime Himalayan-Tibetan Plateau snowpack on the onset of the Indian summer monsoon in coupled seasonal forecasts, Clim. Dyn., 47, 2709–2725, 2016.

Shao, Y., Wyrwoll, K. H., Chappell, A., Huang, J., Lin, Z., McTainsh, G. H., Mikami, M., Tanaka, T. Y., Wang, X., and Yoon, S.: Dust cycle: an emerging core theme in Earth System Science, Aeolian Res., 2, 181–204, 2011.

Shi, Z., and Liu, X.: Distinguishing the provenance of fine-grained eolian dust over the Chinese Loess Plateau from a modelling perspective, Tellus, 63B, 959-970, 2011.

Shi, Z., Liu, X., An, Z., Yi, B., Yang, P., and Mahowald, N.: Simulated variations of eolian dust from inner Asian deserts at the mid-Pliocene, last glacial maximum, and present day: contributions from the regional tectonic uplift and global climate change, Clim. Dyn., 37, 2289-2301, 2011.

Solmon, F., Nair, V.S., and Mallet, M.: Increasing Arabian dust activity and the Indian summer monsoon, Atmos. Chem. Phys, 15, 80519–8064, 2015.

Su, L., and Toon, O. B.: Saharan and Asian dust: Similarities and differences determined by CALIPSO, AERONET, and a coupled climate-aerosol microphysical model. Atmos. Chem. Phys., 11, 3263–3280, https://doi.org/10.5194/acp-11-3263-2011, 2011.

Sun, H., Pan, Z., and Liu, X.: Numerical simulation of spatial-temporal distribution of dust aerosol and its direct radiative effects on East Asian climate, J. Geophys. Res., 117, D13206, doi:10.1029/2011JD017219, 2012.

Takemura, T., Egashira, M., Matsuzawa, K., Ichijo, H., O′ishi, R., and Abe-Ouchi, A.: A simulation of the global distribution and radiative forcing of soil dust aerosols at the Last Glacial Maximum. Atmospheric Chemistry and Physics, 9, 3061–3073, https://doi.org/10.5194/acp-9-3061-2009, 2009.

Tang, Y., Han, Y., Ma, X., and Liu, Z.: Elevated heat pump effects of dust aerosol over northwestern China during summer, Aeolian Res. 23, 95–104, 2018.

Tegen, I., and Lacis, A. A.: Modeling of particle size distribution and its influence on the radiative properties of mineral dust aerosol, J. Geophys. Res., 101(D14), 19237–19244, 1996.

Toon, O. B., McKay, C. P., Ackerman, T. P., and Santhanam, K.: Rapid calculation of radiative heating rates and photodissociation rates in inhomogeneous multiple scattering atmospheres, J. Geophys. Res., 94(D13), 16287–16301, 1989.

Uno, I., Eguchi, K., Yumimoto, K., Takemura, T., Shimizu, A., Uematsu, M., Liu, Z., Wang, Z., Hara, Y., and Sugimoto, N.: Asian dust transported one full circuit around the globe, Nature Geosci., 2, 557–560, 2009.

Vernekar, A. D., Zhou, J., and Shukla, J.: The effect of Eurasian snow cover on the Indian monsoon, J. Clim., 8, 248–266, 1994.

Vinoj, V., Rasch, P. J., Wang, H., Yoon, J., Ma, P., Landu, K., and Singh, B.: Short-term modulation of Indian summer monsoon rainfall by West Asian dust, Nature Geosci., 7, 308–313, 2014.

Wang, Z., Wu, R., Chen, S., Huang, G., Liu, G., and Zhu, L.: Influence of western Tibetan Plateau summer snow cover on East Asian summer rainfall, J. Geophys. Res.: Atmos., 123, 2371–2386, 2017.

Wu, G., Liu, Y., He, B., Bao, Q., Duan, A., and Jin, F.: Thermal Controls on the Asian Summer Monsoon. Sci. Rep., 2, 404, doi: https://doi.org/10.1038/srep00404, 2012.

Xie, X. N., Liu, X. D., Che, H. Z., Xie, X. X., Wang, H. L., Li, J. D., Shi, Z. G., and Liu, Y.: Modeling East Asian dust and its radiative feedbacks in CAM4-BAM, J. Geophys. Res. Atmos., 123, 1079–1096, https://doi.org/10.1002/2017JD027343, 2018a.

Xie, X. N., Liu, X. D., Che, H. Z., Xie, X. X., Li, X. Z., Shi, Z. G., Wang, H. L., Zhao, T. L., and Liu, Y.: Ratiative feedbacks of dust-in-snow over East Asia in CAM4-BAM, Atmos. Chem. Phys., 18, 12683–12698, 2018b.

Xu, B. Q., Cao, J., Hansen, J., Yao, T., Joswiak, D. R., Wang, N., Wu, G.,Wang, M., Zhao, H., Yang,W., Liu, X., and He, J.: Black soot and the survival of Tibetan glaciers, P. Natl. Acad. Sci. USA, 106(52), 22114–22118, doi:10.1073/pnas.0910444106, 2009.

Yanai, M., C. Li, and Z. Song.: Seasonal heating of the Tibetan Plateau and its effects on the evolution of the Asian summer monsoon, J. Meteor. Soc. Japan, 70(1B), 319–351, 1992.

Yasunari, T. J., R. D. Koster, K.-M. Lau, T. Aoki, Y. C. Sud, T. Yamazaki, H. Motoyoshi, and Y. Kodama: Influence of dust and black carbon on the snow albedo in the NASA Goddard Earth Observing System version 5 land surface model, J. Geophys. Res., 116, D02210, doi: 10.1029/2010JD014861, 2010.

Yasunari, T. J., Koster, R. D., Lau, W. K. M., and Kim, K.-M.: Impact of snow darkening via dust, black carbon, and organic carbon on boreal spring climate in the Earth system, J. Geophys. Res. Atmos., 120, 5485–5503, doi:10.1002/2014JD022977, 2015.

Zhang, D. F., Zakey, A. S., Gao, X. J., Giorgi, F., and Solmon, F.: Simulation of dust aerosol and its regional feedbacks over East Asia using a regional climate model, Atmos. Chem. Phys., 9, 1095–1110, doi:10.5194/acp-9-1095-2009, 2009.

Zhang, X. Y., Arimoto, R., and An, Z. S.: Dust emission from Chinese desert sources linked to variations in atmospheric circulation, J. Geophys. Res., 102(DD23), 28, 041–28, 047, 1997.

Zhang, Y., Kang, S., Sprenger, M., Cong, Z., Gao, T., Li, C., Tao S., Li, X., Zhong, X., Xu, M., Meng, W., Neupane, B., Qin, X., and Sillanpää, M.: Black carbon and mineral dust in snow cover on the Tibetan Plateau, The Cryosphere, 12, 413-431, 2018.

Zhang, Y., Wu, G., Liu, Y., and Guan, Y.: The effects of asymmetric potential vorticity forcing on the instability of South Asia High and Indian summer monsoon onset, Sci. Chi. Earth Sci., 57, 337-350, 2014.

Zhao, C., Hu, Z., Qian, Y., Leung, L., Huang, J., Huang, M., Jin, J., Flanner, M. G., Zhang, R., Wang, H., Yan, H., Lu, Z., and Streets, D. G.: Simulating black carbon and dust and their radiative forcing in seasonal snow: a case study over North China with field campaign measurements. Atmos. Chem. Phys., 14, 11475–11491, 2014.

Zhao, T. L., Gong, S. L., Zhang, X. Y., Blanchet, J. P., McKendry, I. G., and Zhou, Z. J.: A simulated climatology of Asian dust aerosol and its trans-Pacific transport, Part I: Mean climate and validation. J. Clim. 19, 88–103, 2006.

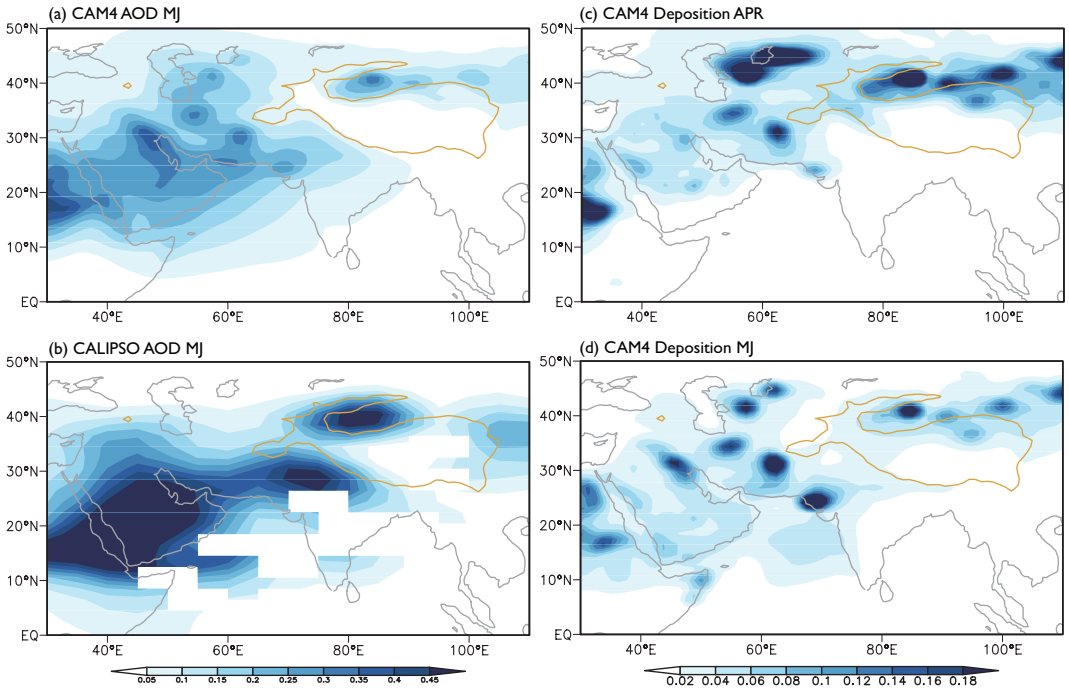

Figure 1. Averaged dust aerosol optical depth over Asia for May and June in CAM4 (a) and in Cloud-Aerosol Lidar and Infrared Pathfinder Satellite Observation (CALIPSO)-retrieved data for 2007-2011 (b); and mean dust deposition flux including both dry and wet deposition for April (c) (kg/m^2/yr) and for May and June (d). Yellow line shows the profile of Tibetan Plateau above 2500 m.

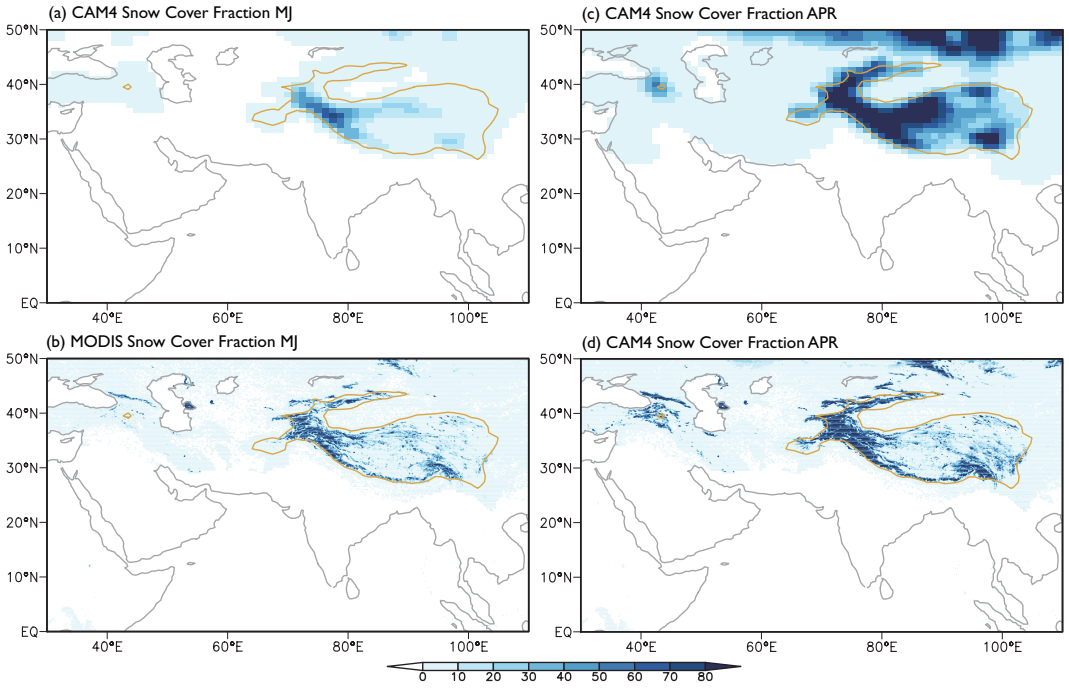

Figure 2. Snow cover fraction (%) over Asia in CAM4 (a, c) and in Moderate Resolution Imaging Spectroradiometer (MODIS)-retrieved observation (b, d) for May to June, and for April, respectively. Yellow line shows the profile of Tibetan Plateau above 2500 m.

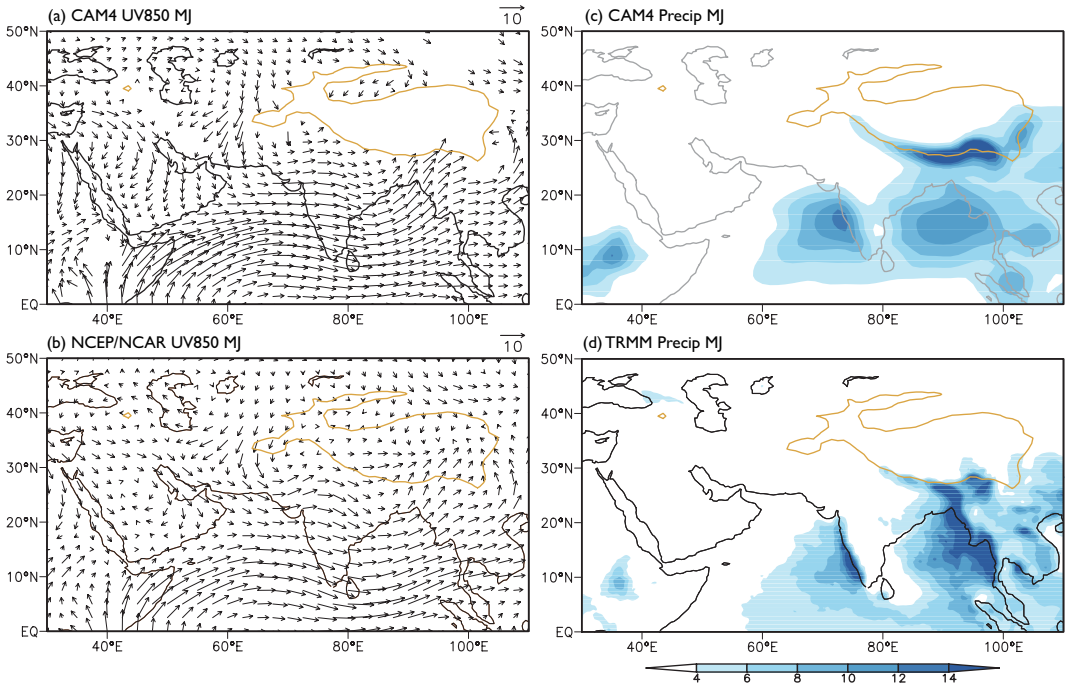

Figure 3. Averaged 850 hPa wind vectors (m s^{-1}) over Indian monsoon region for May and June in CAM4 (a) and in National Centers for Environmental Prediction/National Center for Atmospheric Research (NCEP/NCAR) reanalysis data (b); and precipitation rates (mm day^{-1}) for May and June in CAM4 (c) and in Tropical Rainfall Measuring Mission (TRMM)-retrieved data (d). Yellow line shows the profile of Tibetan Plateau above 2500 m

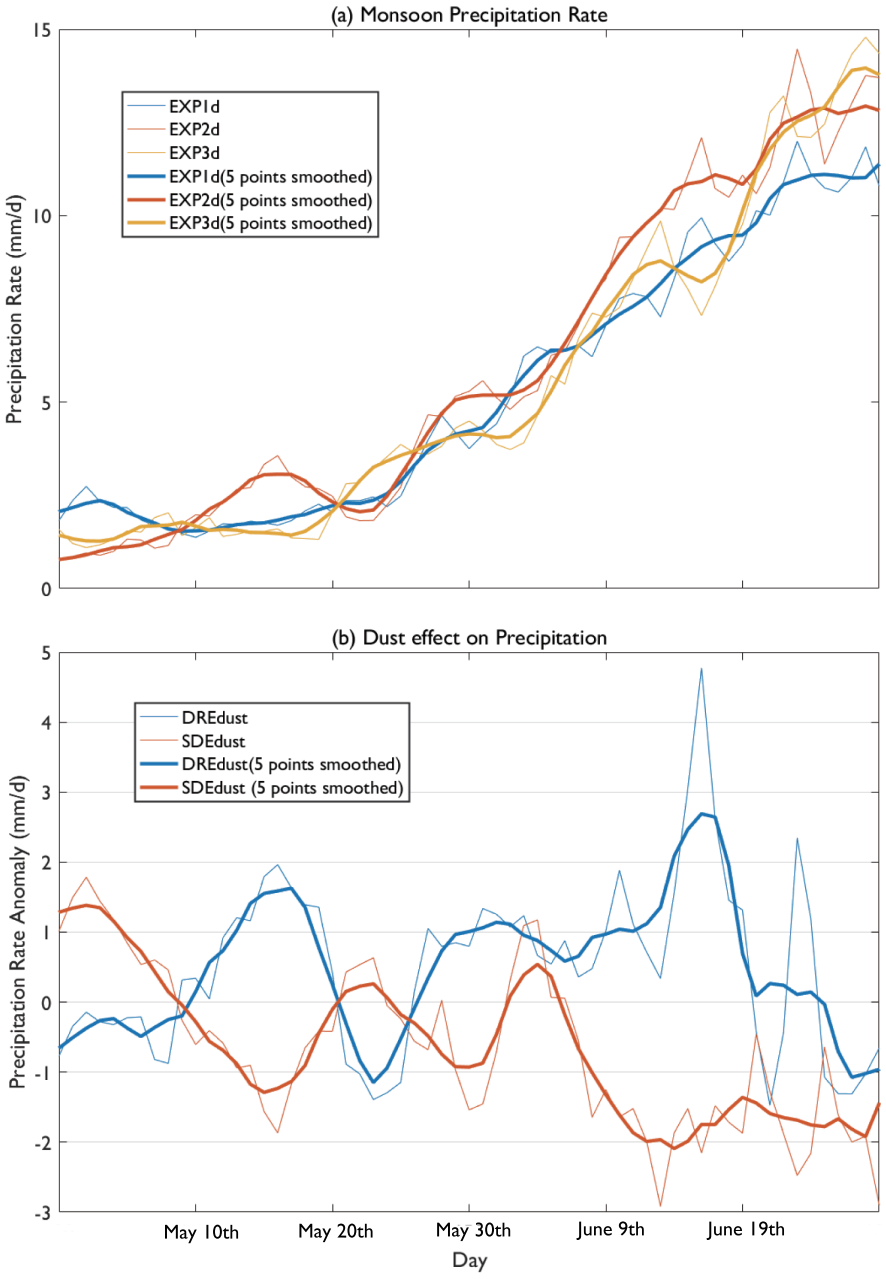

Figure 4. Daily precipitation rates (mm day^{-1}), averaged for monsoon area (10-25°N, 65-100°E), during May and June in three experiments (a) and the differences (mm day^{-1}) induced by snow-darkening effect and direct radiative effect of dust (b). Thin lines show the daily values and thick ones are 5-day smoothed. In b, red lines donate snow-darkening effect and blue lines donate direct radiative effect.

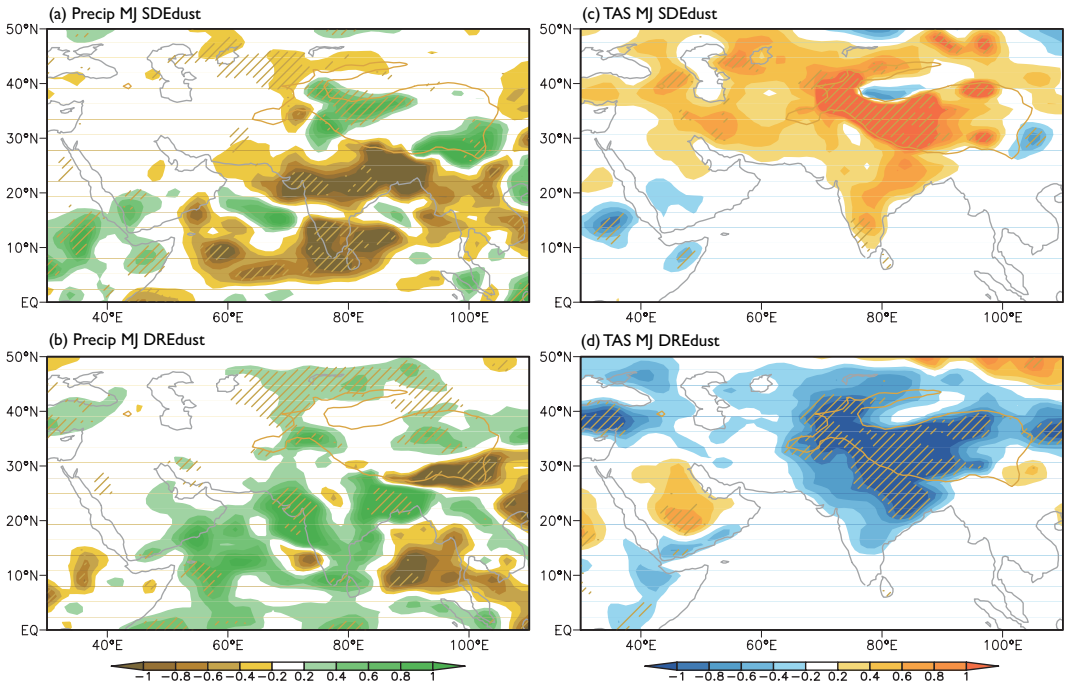

Figure 5. Spatial distribution of changes in precipitation rates (a, b, mm day^{-1}) and surface air temperature (c, d, °C) in May and June induced by snow-darkening effect (top) and direct radiative effect of dust (bottom), respectively. Oblique lines indicate differences significant at 95% confidence level. Yellow line shows the profile of Tibetan Plateau above 2500 m.

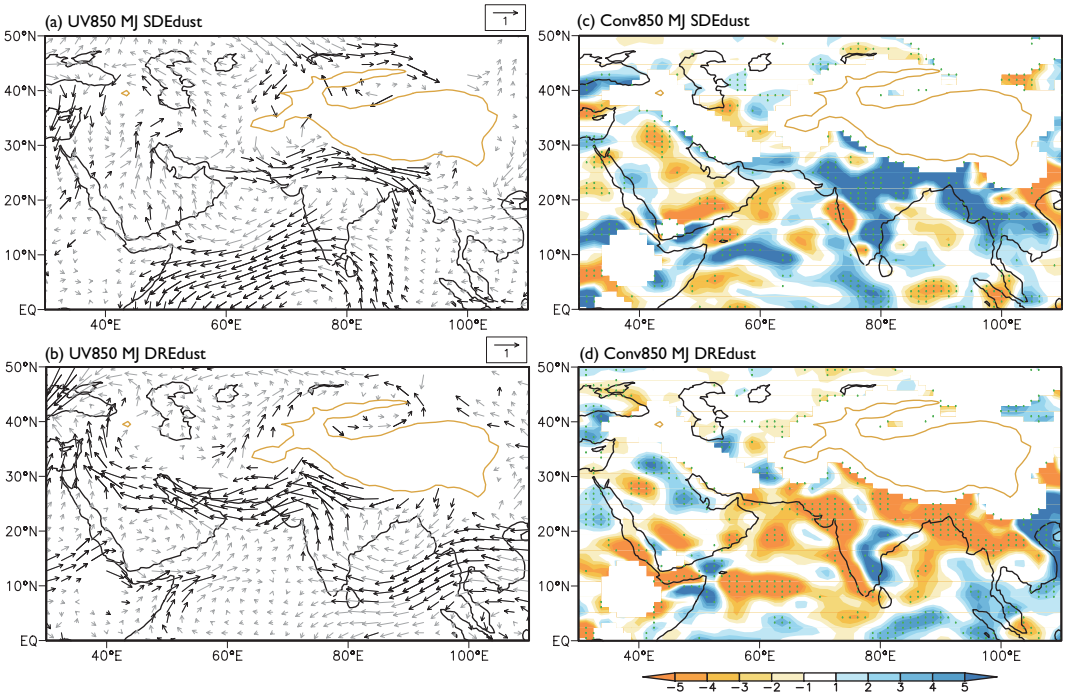

Figure 6. Spatial distribution of changes in 850 hPa wind vectors (a, b, m s^{-1}) and moisture convergence (c, d, g s kg^{-1} m^{-1}) in May and June induced by snow-darkening effect (top) and direct radiative effect of dust (bottom), respectively. Positive values in c and d means divergence anomaly and negative means convergence. Black arrows and green dots indicate differences significant at 90% confidence level. Yellow line shows the profile of Tibetan Plateau above 2500 m.

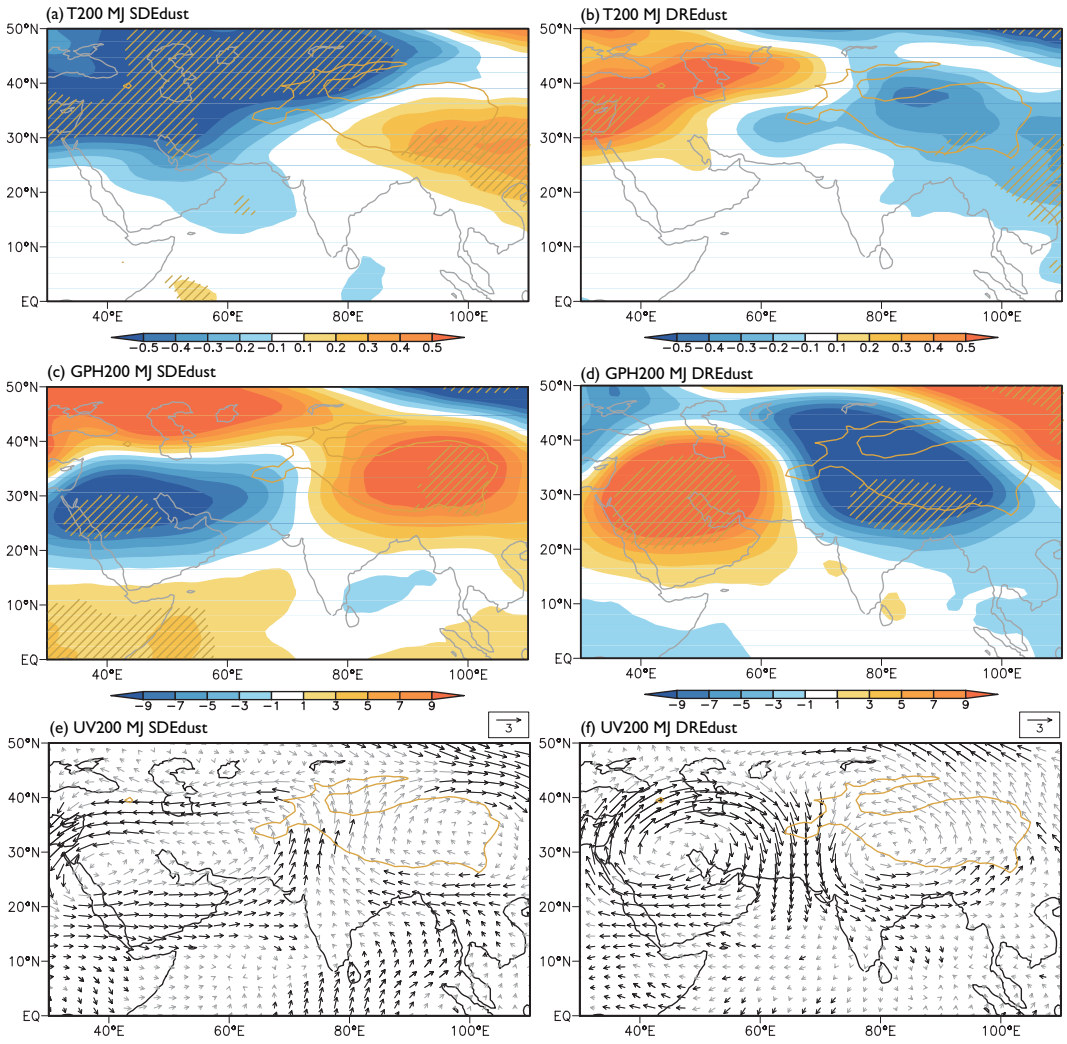

Figure 7. Spatial distribution of changes in 200 hPa temperature (a, b, °C), geopotential height (c, d, gpm) and wind vectors (e, f, m s^{-1}) in May and June induced by snow-darkening effect (left) and direct radiative effect of dust (right), respectively. Oblique lines and black arrows indicate differences significant at 90% confidence level. Yellow line shows the profile of Tibetan Plateau above 2500 m.

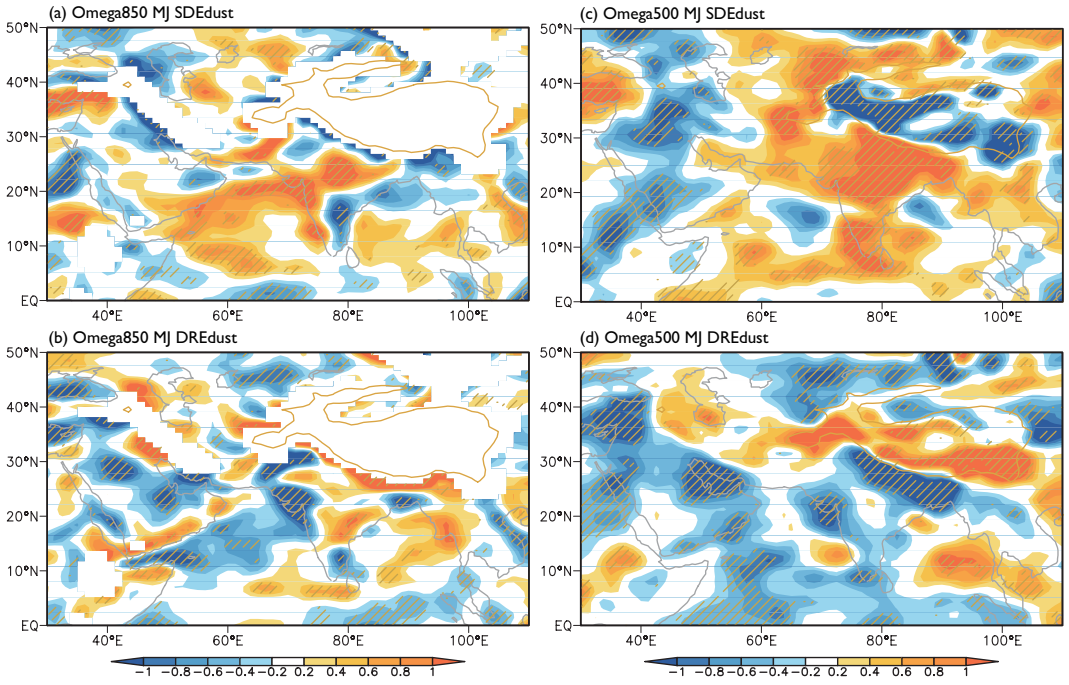

Figure 8. Spatial distribution of changes in 850 hPa (a, b) and 500 hPa (c, d) vertical wind speed ($\times 100$, Pa s^{-1}) in May and June induced by snow-darkening effect (top) and direct radiative effect of dust (bottom), respectively. Negative values indicate upward flow and positive indicate downward flow. Oblique lines indicate differences significant at 95% confidence level. Yellow line shows the profile of Tibetan Plateau above 2500 m.

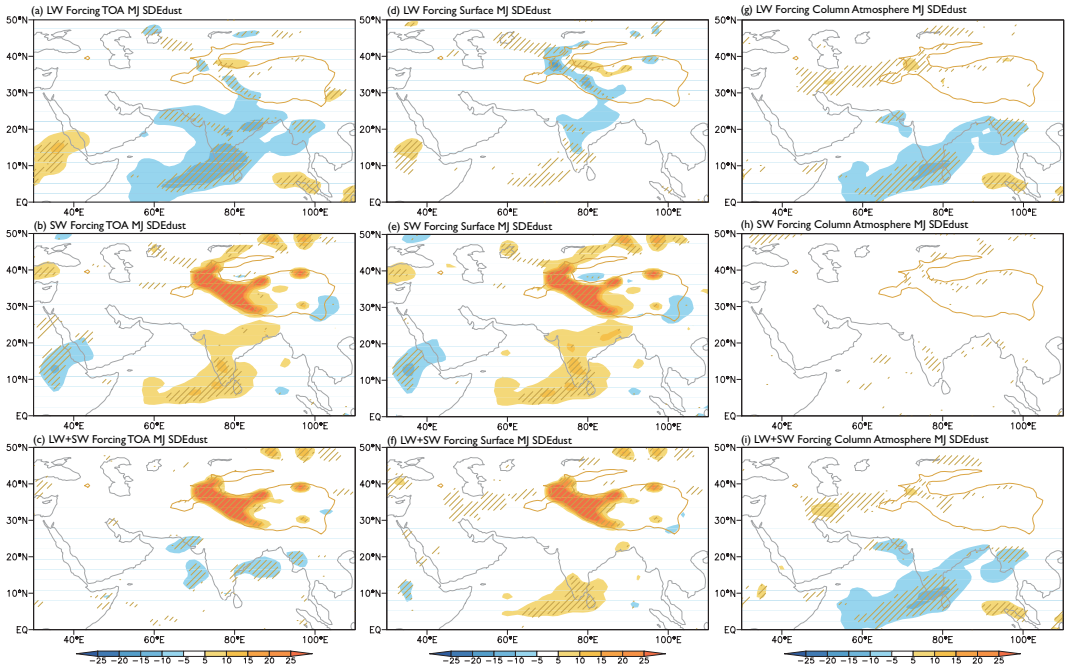

Figure 9. Changes in longwave (top, W m^{-2}), shortwave (middle, W m^{-2}) and net (longwave+shortwave, bottom, W m^{-2}) radiative fluxes during May and June by snow-darkening effect of dust for the top of atmosphere (TOA, a-c), the surface (d-f) and the column atmosphere (g-i). Oblique lines indicate differences significant at 95% confidence level. Yellow line shows the profile of Tibetan Plateau above 2500 m.

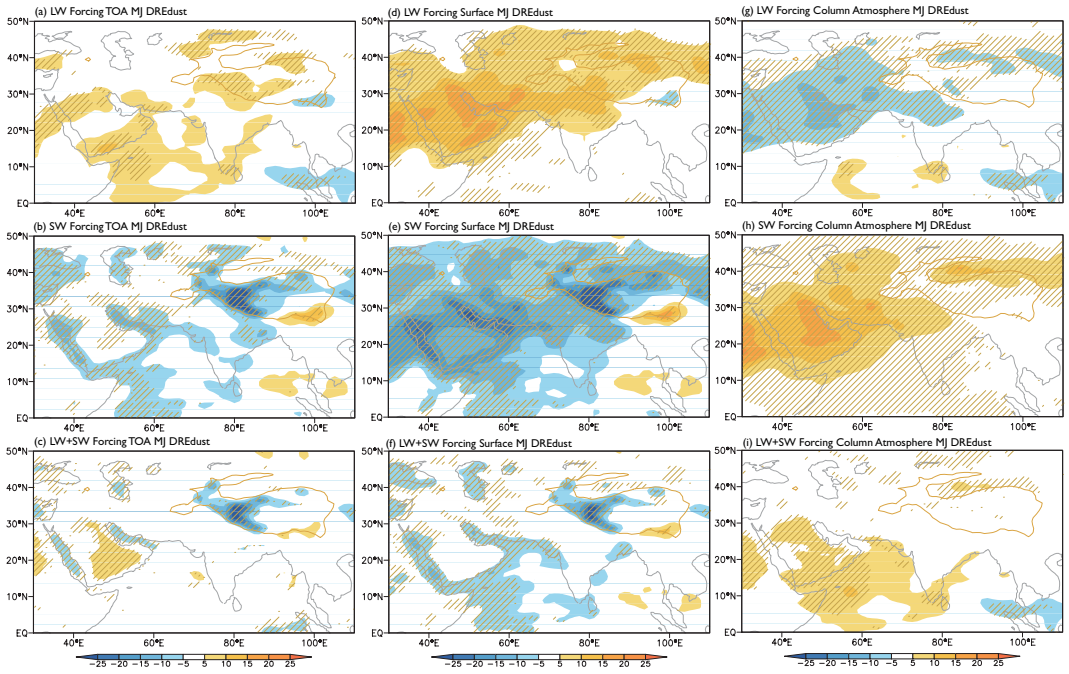

Figure 10. Similar with Figure 9, but for direct radiative effect of dust.

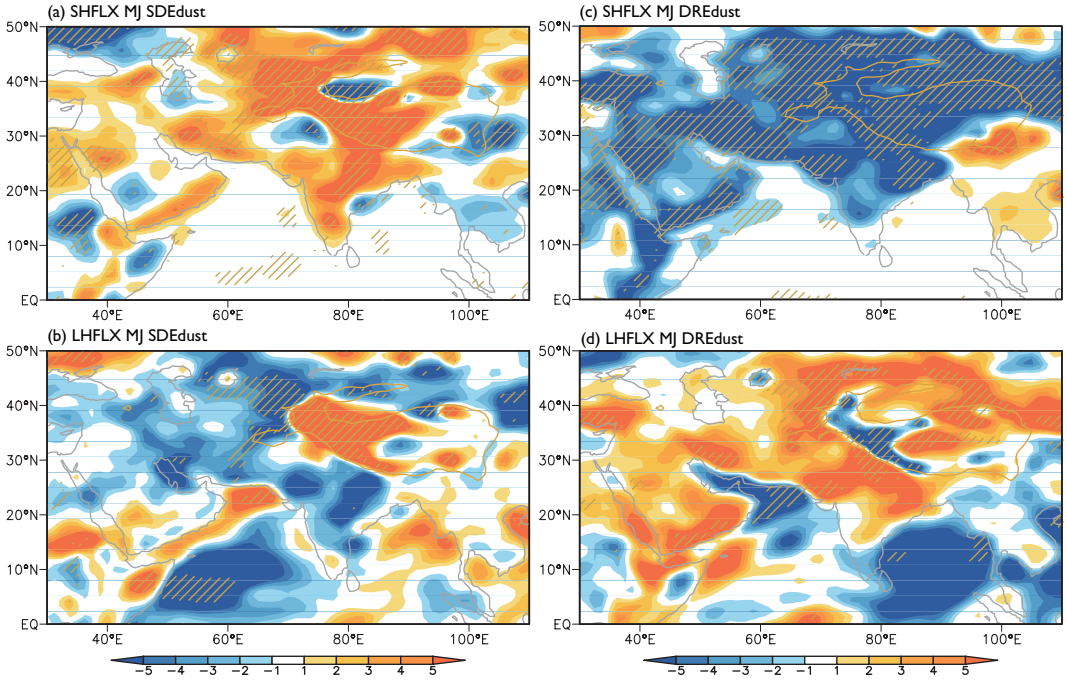

Figure 11. Changes in surface sensible and latent heat fluxes (W m^{-2}) in May and June induced by snow-darkening effect (a, b) and direct radiative effect of dust (c, d), respectively. Oblique lines indicate differences significant at 95% confidence level. Yellow line shows the profile of Tibetan Plateau above 2500 m.

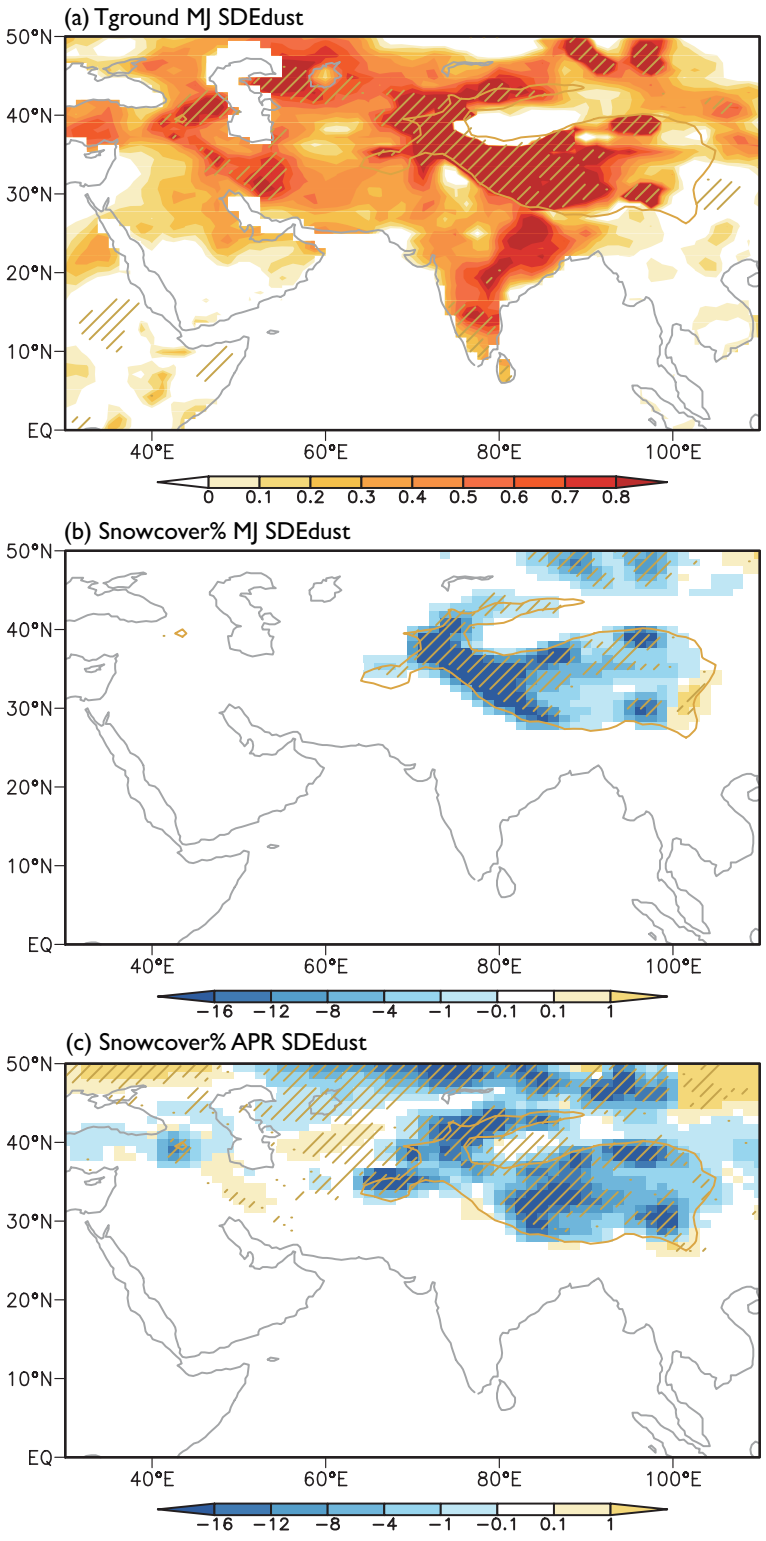

Figure 12. Changes in surface ground temperature in May and June (°C, a) and snow cover fraction during May to June (%, b) and April (%, c) induced by snow-darkening effect. Oblique lines indicate differences significant at 95% confidence level. Yellow line shows the profile of Tibetan Plateau above 2500 m.

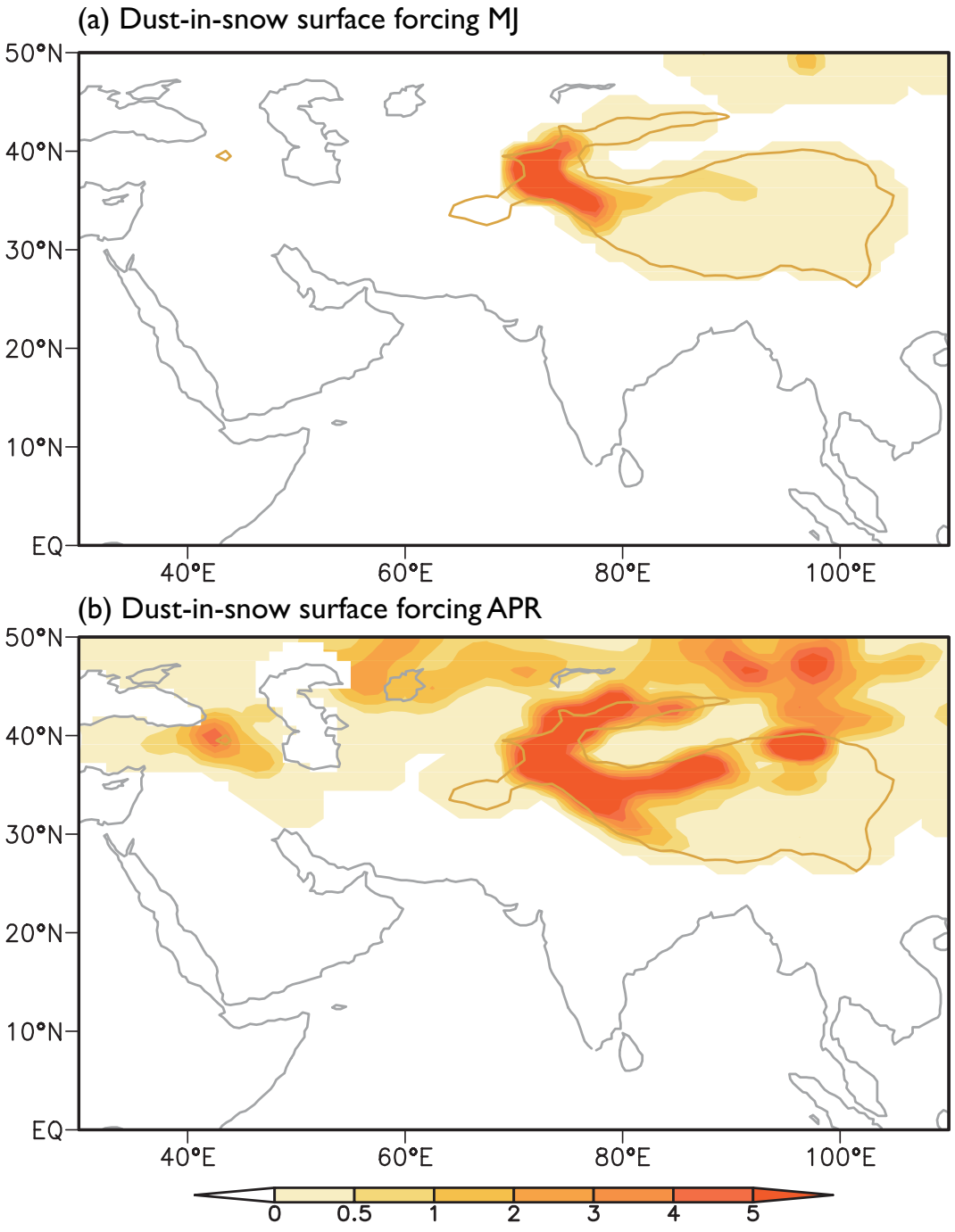

Figure 13. Surface forcing of dust-in-snow during May to June (W m^{-2}, a) and April (W m^{-2}, b). Yellow line shows the profile of Tibetan Plateau above 2500 m.

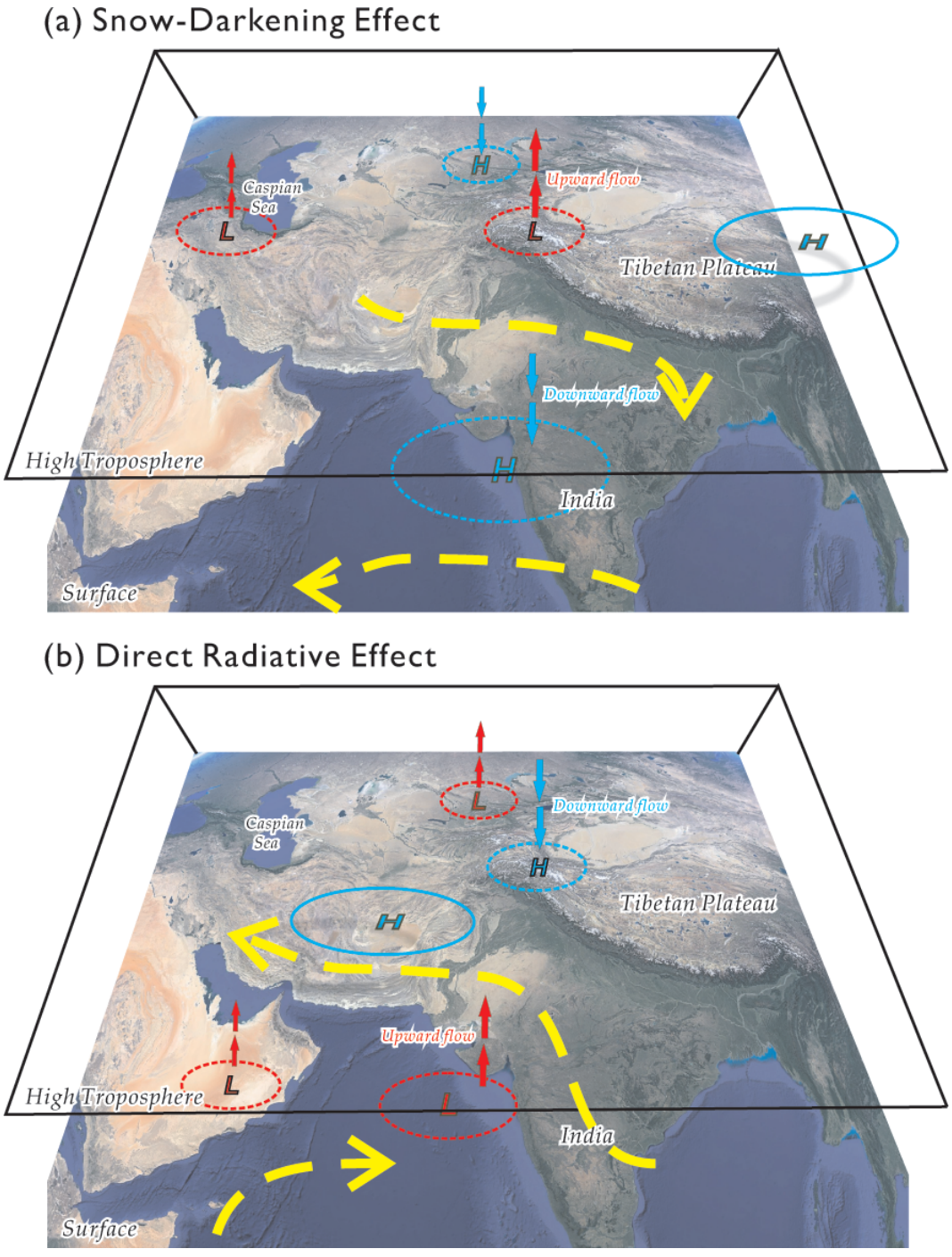

Figure 14. Schematic diagrams showing the forcing mechanisms of snow-darkening effect (a) and direct radiative effect (b) of mineral dust on Indian monsoon during the onset. The circles and abbreviations in them denote the anomalous pressure centers: high pressure (blue), low pressure (red), near surface (dashed) and high troposphere (solid). The red and blue arrows indicate the upward and downward air flows, respectively, and the yellow ones present the differences in horizontal winds.